Raytracing for Parallax 3-D Display

Szymon Jakubczak*
MIT CSAIL

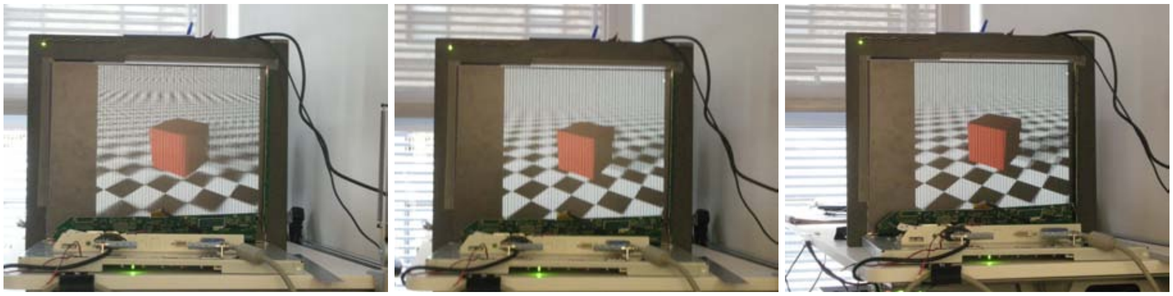

Figure 1: ***Left:*** *One view of a synthetic scene on a prototype display.* ***Center:*** *Same scene after super-sampling.* ***Right:*** *Same scene at different viewing angle.*

Abstract

Automultiscopic displays deliver stereoscopic views without glasses to arbitrary positions within the viewing zone. We present such a display realized using two stacked programmable LCD displays. This paper considers the light-field projected from this display and explores how to synthesize desired light-fields from 3-D models using ray tracing. In particular, we examine the relation of simulated ray geometry to the angular resolution, depth of field and target view zone size of the resulting light-field.

Keywords: FIXME: 3-d displays, raytracing

1 Introduction

A parallax display presents a different view depending on the viewer's position. This feature enables projection of views of a three-dimensional scene that correspond to the camera position, leading to applications in three-dimensional (3-D) television systems, spatial augmented reality, etc.

Automultiscopic or multi-view autostereoscopic displays offer viewing of stereoscopic images from arbitrary positions without glasses or head-tracking. Such displays are commonly composed of view-dependent subpixels projecting angularly varying color. Three techniques are typically employed to implement such subpixels: parallax barriers, lenticular sheets and integral lens sheets. Of the three, parallax barriers realized using programmable LCD screens offer most flexibility allowing dynamic adjustment of barrier parameters to the projected light-field.

This paper explores a barrier-based automultiscopic display realized using two stacked LCD displays. Recent advancements in LCD resolution made such displays practical and affordable. Parallax LCD displays are shipping from multiple companies, whether realized using lenticulars (Philips WOWvx), parallax barrier (NewSight) or parallax illumination (DTI). Although the optics of barrier displays have been known for over a century [Lippmann 1908], the most widespread approach to mapping light-field data to such displays by directly mapping camera views to view zones (see Fig. 2) results in bad quality of projected image. Specifically, the problem of angular aliasing in such displays has received little attention until recently [Zwicker et al. 2006].

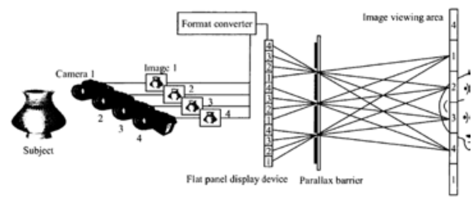

Figure 2: *Direct mapping of captured images from multiple cameras to a parallax-barrier display.*

1.1 Contributions

In this paper, we investigate how to synthesize desired light-fields from 3-D models using ray tracing. In particular, we define the ray geometry and parallax barrier parameters to match desired view zone. We show how to adjust the ray geometry to trade depth-of-field for angular span of the scene. Finally, we propose a simple ray-space angular anti-aliasing method which is analog to spatial subsampling in rendering for planar displays. We realize a programmable dual-LCD parallax-barrier display and demonstrate the effect of anti-aliasing on resulting light-field. We discuss calibration and impact of pitch size and barrier mask design on the quality of display.

1.2 Related Work

The concept of autostereoscopy and integral photography has been known for over a century [Lippmann 1908]. In [Isono et al. 1993], the concept of using a programmable LCD-generated parallax barrier is first proposed to implement autostereoscopic display. However, the consideration of benefits is limited to the ability of switching the barrier between slits/pinholes and fully transparent to support 3-D and 2-D display modes. In [Peterka et al. 2008], a programmable parallax barrier is used to create autostereoscopic display that utilizes head tracking to update the projected lightfield to match the viewer's position. In contrast, in this paper we are concerned with tracking-free automultiscopic displays.

The problem of angular resolution of parallax-barrier displays has been analyzed in [Hoshino et al. 1998].

The problem of inter-perspective aliasing in holographic displays has been analyzed geometrically by [Halle 1994]. A method of combating the aliasing by prefiltering in the ray-space has been proposed in [Zwicker et al. 2006].

2 Geometry

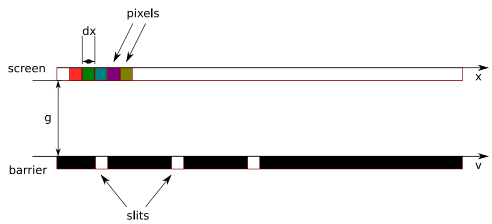

Figure 3: *A horizontal slice of the display. Pixels of the screen are located along the x axis, while the slits are located along a parallel v axis.*

The geometry of the display can be described as in Fig. 3 by the following parameters:

- distance between the barrier and the screen, or gap, g
- location of the slits in the barrier
- resolution of the screen, dx

For simplicity, we consider this parametrization in one horizontal slice of the display. This is acceptable, since the horizontal (and stereo) parallax is of primary interest. In fact, most of the parallax displays use 1-D barriers and are designed to provide horizontal parallax only.

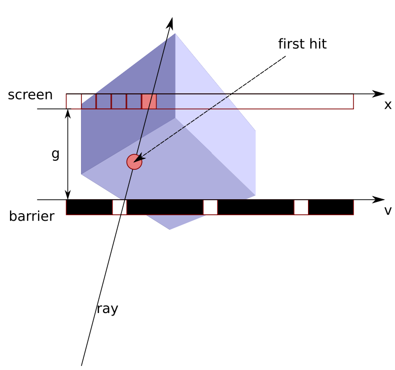

Figure 4: *Projecting rays through virtual slits to determine the color of each screen pixel.*

To synthesize the image to be projected from the screen, we replicate this geometry in our virtual ray tracing model. The slits and pinholes are modeled as points in 3-D. To determine the color of particular pixel on the screen, we cast a ray from the associated slit through the pixel and trace it through the scene, as illustrated in Fig. 4. The first intersection, or hit, determines the color of the pixel. Thus, to support parallax barrier displays, a typical ray tracer needs only to implement a new type of *camera* (which determines the geometric ray for each rendered pixel). Note that we are ignoring here the fact that each pixel of an LCD display is actually composed of horizontally aligned RGB subpixels. We address this issue later.

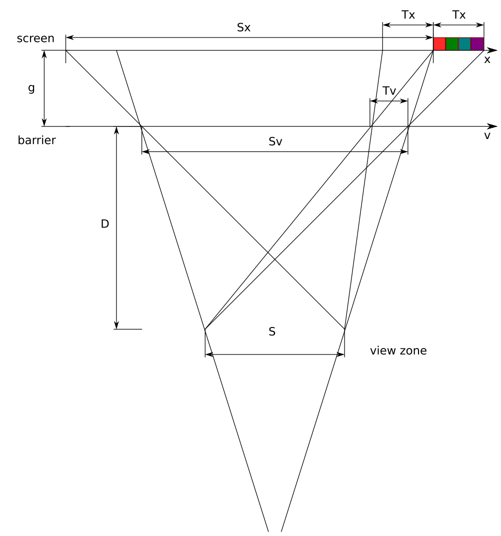

Figure 5: *The design view zone and gap determines the minimum slit spacing.*

2.1 Barrier Design

To determine which slit is associated with each pixel, we need to consider the desired view zone. This a simple geometric argument presented in Fig. 5. If the view zone (defined as locations where the correctly projected view has maximum angle) is parallel to the screen, the slit arrangement that maximizes screen efficiency is periodic. The period, Tv, is the minimum distance between slits such that every point of the screen is visible through exactly one slit at any position in the view zone. The relation of the slit period to the width, S, and distance, D, of the view zone is as follows:

$$Tx/Tv = (D+g)/D = (Sx-Tx)/Sv \qquad (1)$$
$$S/Tx = D/g \qquad (2)$$
$$Sv = (Sx-Tx)(D+g)/D \qquad (3)$$

where Tx is the area of the screen committed to each slit. Note how the slit period and the effective screen size Sv must decrease to support shorter viewing distance. On the other hand, if the viewer's position is farther away than D, the view is still correct, as long as it's located in a triangle behind the viewzone.

We use the term *correct* in the sense that each point on the screen is visible only through the associated slit through which the virtual ray was cast. However, because there are no barriers between the slits within the gap, if the viewer's position is outside of the viewzone, each pixel is still visible but through a different slit. The view will appear slightly geometrically distorted but still visually consistent, as long as the viewer is between D and $Dmax = D\frac{S}{Sv-S}$ away from the display. Otherwise, the viewer observes rays that do not map in any geometric way to the traced rays. This happens when two pixels ray traced through a single slit are visible through different physical slits.

Thus inter-slit distance determines the spatial resolution of the resulting image to $Sv/Tv+1$ view-dependent pixels. Considering the resolution of the screen, dx, one can observe that in this arrangement, there is Tx/dx possible distinct views in the view zone. Note that the total resolution of the screen is obviously divided between the angular and spatial resolution, since $\frac{Tx}{dx}\frac{Sv+Tv}{Tv} = \frac{Sx}{dx}$.

2.2 Perspective

The geometric argument above suggests that the view should be visually accurate as long as the viewer's position remains within the view zone. However, this reasoning can be only applied to the axis of the parallax. If the display does not offer parallax in the vertical direction, then we must ensure visual consistency between the horizontal and vertical perspective projections by adjusting the ray tracing camera in its y dimension. In a simple perspective camera for ray tracing, all rays should intersect at the camera origin, which is a single point. In a one-axis parallax perspective camera, all rays would intersect at the line of the design view zone, as shown in Fig. 6. If the viewer moves away from the view zone, the perspective in the y dimension remains fixed and no longer matches the proper view-dependent perspective in the x dimension.

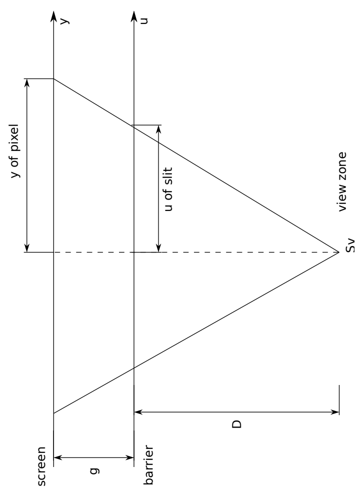

Figure 6: *Ray tracing adjusted for perspective in the y dimension which is absent of parallax.*

2.3 Physical Display vs. Virtual Camera

So far, we have assumed that the virtual ray casting camera matches the geometry of the display. However, this needs not be the case by design. For instance, by adjusting the virtual gap, g, we can control the range of virtual depth of the scene and the angular span. Bigger simulated gap translates to smaller range of depth and smaller angular span (i.e., less differing views). Similarly, by adjusting the virtual perspective distance discussed in the previous section, we can affect the perceived distance of the viewer to the projected light-field.

Rather than trying to match the geometry exactly, we can simplify the problem by assuming only that the virtual Tv/Tx match the simulated perspective distance D, and adjusting D and g to achieve desired visual effect.

2.4 Aliasing

Although the geometric argument in the previous section suggests that the view should be correct, as long as the viewer's position remains within the view zone, since the pixels are visible through the intended slits, the discrete nature of the screen process results in limited of angular resolution which causes angular or inter-perspective aliasing [Halle 1994]. Another way to consider the resolution of parallax display is in the light-field parametrization as in [Zwicker et al. 2006]. Each point in the graph corresponds to a single ray, i.e. one pixel observed through its corresponding slit and is described by the intersections with the x and t axes. as shown in Fig. 7. Thus both the spatial and angular sampling frequency is limited.

If the light-field of the virtual scene exhibits higher frequencies than the sampling frequency, the viewer will observe aliasing effects. Aliasing in space is the well known effect of ghost patterns in high-frequency textures. Aliasing in frequency manifests itself by distinguishable ghost views observed when the viewer is positioned between two "correct" positions. As analyzed by [Halle 1994] geometrically, and by [Zwicker et al. 2006] in terms of display bandwidth, the *depth of field* of the display is the range that can be reproduced at maximum spatial resolution. Given our geometry, the depth of field equals $|z| = Tv/dx$. The spatial frequency supported at depth $z > |z|$ (where $z = 0$ at the barrier) is reduced by a factor $|z|/z$.

We can affect effective depth of field of the display, by simulating a viewing distance and display gap that do not reflect the physical setup. This corresponds to *baseline scaling* described in [Zwicker et al. 2006]. This allows us to improve depth of field at the cost of reducing the observable parallax effect, i.e. the scene appears more flat to the viewer.

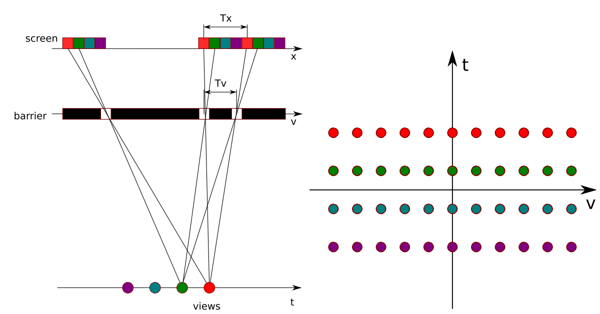

Figure 7: *Two-plane parametrization of the lightfield projected from the display. Each point in the $v-t$ space corresponds to one simulated ray.*

We implement a simple solution to anti-aliasing: super-sampling, see Fig. 8. We cast multiple sub-rays through each slit-pixel pair and take their average to determine the pixel color. For our experiments, we used jittered sampling, where the samples are distributed uniformly within the pixel but with small random offsets.

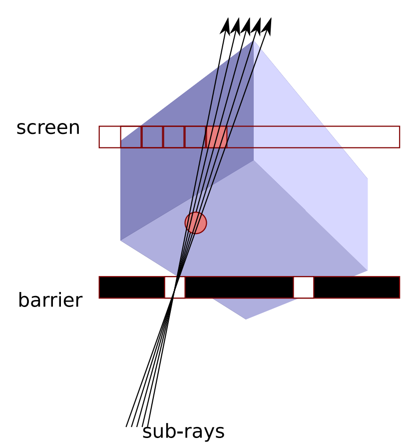

Figure 8: *Super-sampling of the light-field by sub-rays.*

3 Physical Display

We have built a physical prototype of the display by removing backlight diffuser from an LCD display and putting the LCD glass container This creates an air gap of around 3mm between the two LCD screens.[1] The LCD display glass pane is covered from one side via a polarizer+diffuser foil which has not been removed. This lead to more significant cross-talk between perspectives and fewer independent views than the designed 9.

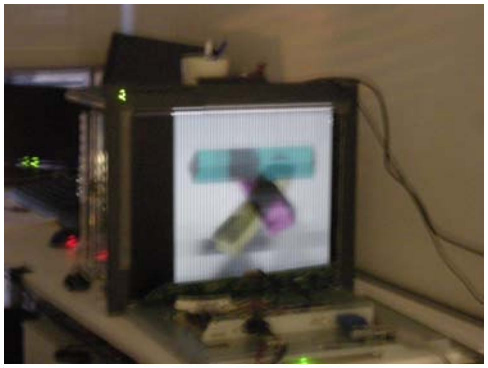

Figure 9: *The physical prototype.*

3.1 Calibration

Rather than measuring the gap and pitch of the screen, a simple calibration routine was employed. Displaying periodic white-on-black slits on both screens and varying the period we could find a ratio of frequencies such that the view becomes as uniformly white in one viewing position and black in all others (until the view wraps around). Due to the sub-pixel nature of both LCDs, the view does not become uniformly white, instead slight rainbow coloring was noticeable. Ideally, the resulting periods Tx and Tv would be both integer number of pixels. Since it was impossible to achieve satisfactory calibration with such periods, we used integer period on the screen and simple anti-aliasing for the slits in the barrier. However, in the barrier-before-screen configuration $Tv < Tx$ which results in the anti-aliased slits being significantly wider than the pixels in the screen, causing further inter-perspective cross-talk and loss of number of views. Instead, in our prototype the roles of the LCDs were inverted, with the screen being displayed in front and the slit barrier acting as parallax illumination in the back. (Note, this requires small adjustment in the ray tracing model.)

4 Results

4.1 Aliasing and Super-sampling

In Fig. 10, we show the results on a simple scene of a box levitating above checkerboard texture. Note that without super-sampling, the aliasing is significant, leading to familiar Moiré effects at some depths. In Fig. 11, we show the same scene super-sampled 16 times ($4\times$ in each angle). Observe that the further away from the depth of field of the display the more blurred the scene appears.

In Fig. 12 we demonstrate the aliasing present even without spatially periodic textures. Visible are the ghosts of multiple shadows on the zoomed portion. In fig. 13 the super-sampled shadows become blurred, since they are beyond the depth of field.

[1]For a short period, a company SynthaGram manufactured a stacked LCD display that allowed dynamic barriers [Peterka et al. 2008], but it seems they are no longer in production.

4.2 Perspective

In Fig. 14 we demonstrate the effect of perspective (virtual distance from the screen) on the resulting image. When the virtual $D = \inf$, each view appears orthographic. This amplifies the loss of angular resolution for depths away from the screen, and substantial inter-perspective aliasing.

4.3 Different Masks

We have experimented with barrier patterns (or rather parallax illumination in our case) other than vertical slits. Diagonal slants (Fig. 15) offer more perceptually uniform illumination at the price of artificial parallax when the viewer shifts position in the y dimension. However, the horizontal parallax remains intact. Wiggling slits (Fig. 16) reduce apparent periodicity of the mask, but are susceptible to complete loss of parallax if the viewer shifts vertical position sufficiently to misalign the physical barrier with the expected (virtual) barrier.

In both cases, the major hindrance to barrier pattern design was the fact that the barrier needs to be stretched during calibration. The simple anti-aliasing employed in the resizing leads to noticeable periodic patterns in light intensity. We have also experimented with randomly jittered periodic mask, but observed no significant benefit in image quality. The side-effect of randomness in the mask is that when the viewer moves out of the view zone, the parallax is lost completely. This effect is due to the fact that a such mask is aperiodic and therefore a shift of one slit does not produce a proper barrier as in the case of periodic masks.

5 Conclusion

In this paper, we discussed how to synthesize desired light-fields from 3-D models using ray tracing. We proposed a simple ray-space angular anti-aliasing method which is analog to spatial sub-sampling in rendering for planar displays. We realized a programmable dual-LCD parallax-barrier display and demonstrated the effect of anti-aliasing on resulting light-field.

References

HALLE, M. W. 1994. Holographic stereograms as discrete imaging systems. In *SPIE*.

HOSHINO, H., OKANO, F., ISONO, H., AND YUYAMA, I. 1998. Analysis of resolution limitation of integral photography. In *JOSA A*, vol. 15.

ISONO, H., YASUDA, M., AND SASAZAWA, H. 1993. Autostereoscopic 3-d display using lcd-generated parallax barrier. In *Electronics and Communications in Japan (Part II: Electronics)*, vol. 76.

LIPPMANN, G. 1908. La photographie intégrale. In *Comptes Rendus*, vol. 146.

PETERKA, T., KOOIMA, R., SANDIN, D., JOHNSON, A., LEIGH, J., AND DEFANTI, T. 2008. Advances in the dynallax solid-state dynamic parallax barrier autostereoscopic visualization display system. In *IEEE TRANSACTIONS ON VISUALIZATION AND COMPUTER GRAPHICS*, vol. 14.

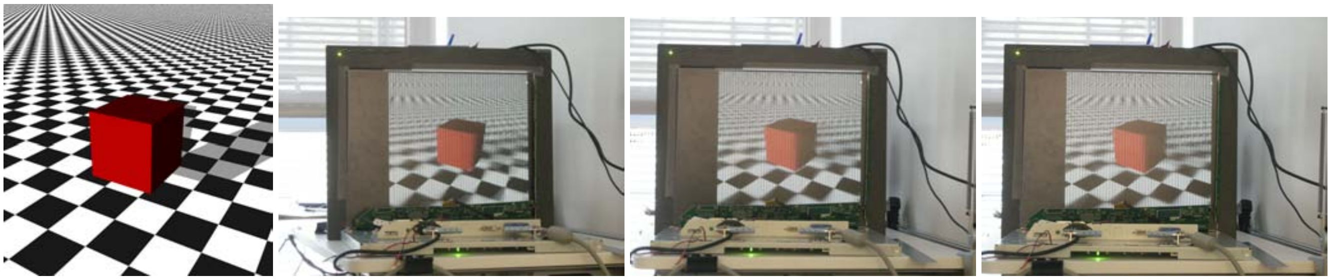

Figure 10: *One view of the scene (anti-aliased at 16 rays per pixel). Views of the parallax display, at one ray per pixel.*

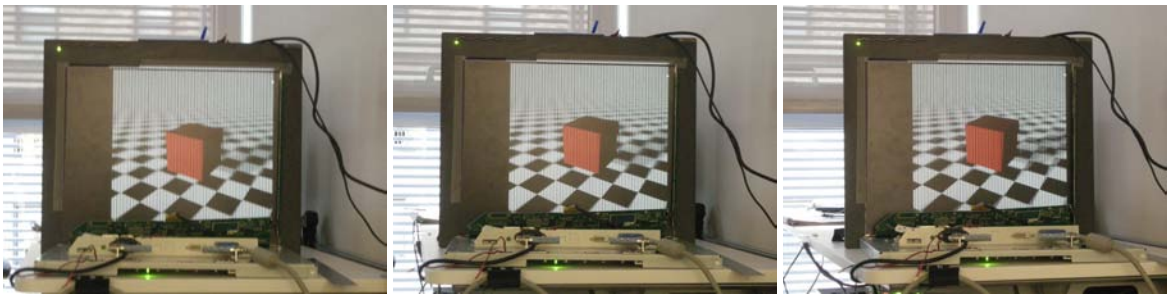

Figure 11: *Views of the super-sampled display, at 16 rays per pixel.*

ZWICKER, M., MATUSIK, W., DURAND, F., AND PFISTER, H. 2006. Antialiasing for automultiscopic 3d displays. In *Eurographics Symposium on Rendering*.

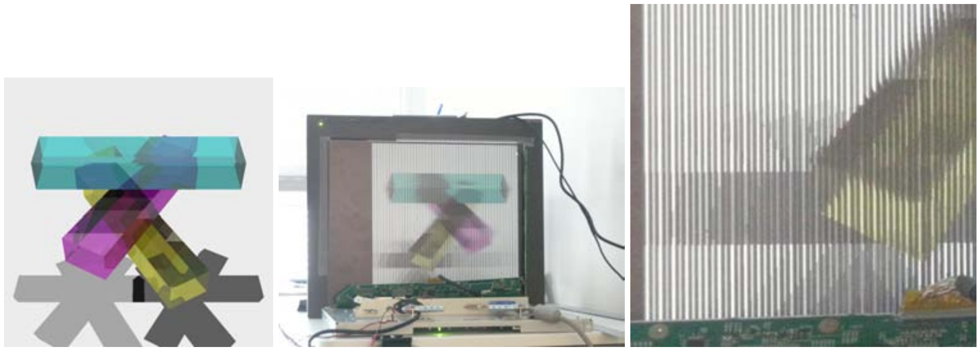

Figure 12: *One ray-traced view of the scene (no anti-aliasing). View of the parallax display and a zoomed portion, at 1 rays per pixel.*

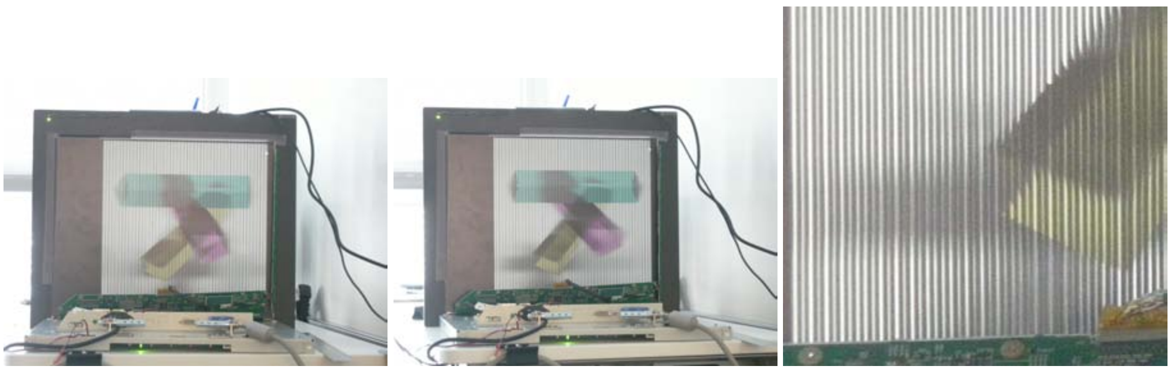

Figure 13: *Views of the super-sampled display and a zoomed portion, at 16 rays per pixel.*

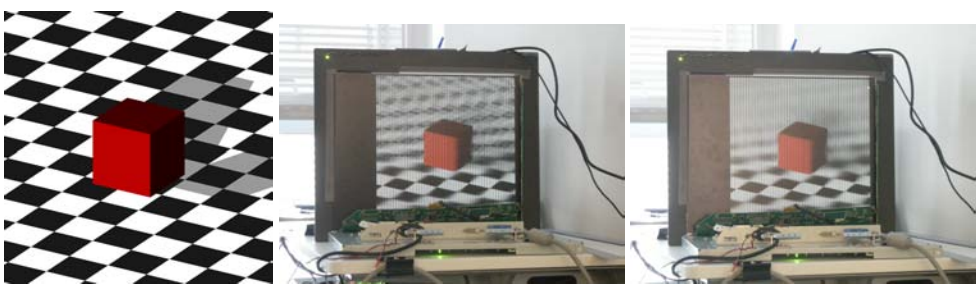

Figure 14: *One view of the scene without perspective. View of the parallax display at 1 and 16 rays per pixel.*

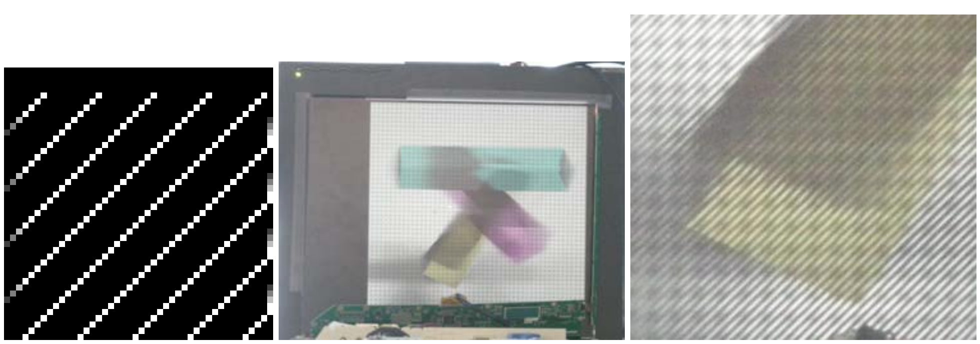

Figure 15: *The slanted mask. View of the parallax display and a zoomed portion.*

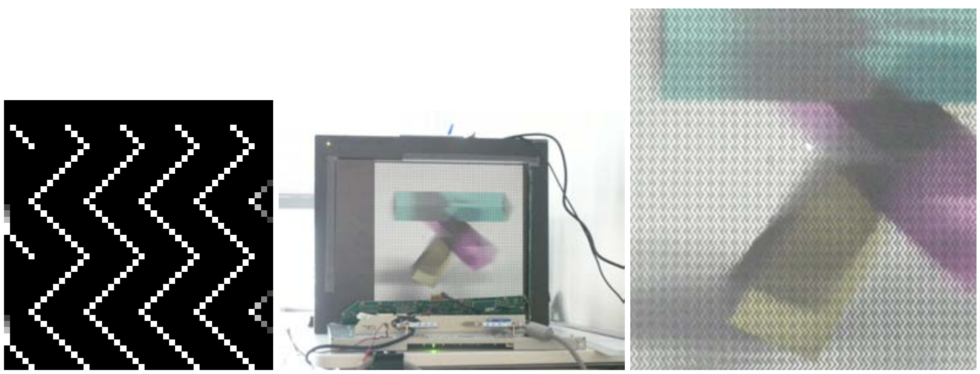

Figure 16: *The wiggling mask. View of the parallax display and a zoomed portion.*